



Effect of partial substitution of Rh catalysts with Pt or Pd during the partial oxidation of methane in the presence of sulphur

S. Cimino^{a,*}, L. Lisi^a, G. Russo^b, R. Torbati^b

^a Istituto Ricerche sulla Combustione, CNR, Italy

^b Dipartimento di Ingegneria Chimica, Università di Napoli Federico II, Italy

ARTICLE INFO

Article history:

Available online 3 March 2010

Keywords:

Sulphur poisoning
Partial oxidation
Steam reforming
Rh
Pt
Pd
Bimetallic
Honeycomb
Methane

ABSTRACT

The effect of the partial substitution of Rh/La–Al₂O₃ monolith catalysts with either Pt or Pd during the catalytic partial oxidation of methane in the presence of H₂S under self-sustained high-temperature conditions was investigated. The catalysts were fully characterized by BET, SEM-EDS, SO₂-TPD and in situ DRIFT spectroscopy of adsorbed CO at room temperature, which was used to study changes on the surface state of Rh before and after exposures to sulphur species at temperatures and conditions close to those expected under actual CPO of methane. Both steady state and transient operation of the CPO reactor were investigated particularly with regards to poisoning/regeneration cycles and low-temperature light-off phase.

The partial substitution of Rh with Pt was shown to reduce the detrimental effect of S, which strongly inhibits the steam reforming reaction on monometallic Rh catalyst. DRIFT experiments indicate that sulphur acts as a selective poison by preferentially adsorbing on smaller well-dispersed Rh crystallites while larger metallic Rh sites are mostly unaffected; the presence of Pt or Pd does not directly influence the way S adsorbs on highly dispersed Rh sites.

© Elsevier B.V. All rights reserved.

1. Introduction

The production of syngas (CO and H₂) via the catalytic partial oxidation (CPO) of methane is an attractive and feasible alternative to steam reforming reaction in the utilisation of the world's abundant natural gas reserves. The syngas can then be converted to clean fuels such as sulphur-free diesel or gasoline by Fischer–Tropsch synthesis. Furthermore, CPO of various hydrocarbons has been proposed as a preliminary conversion stage for hybrid gas turbine catalytic burners [1,2].

Recent results on the effect of sulphur addition during the CPO of methane over Rh-based honeycomb catalysts tested under self-sustained high-temperature condition [3,4] demonstrated that sulphur inhibits the steam reforming (SR) reaction by directly poisoning the active Rh sites. The effect of sulphur poisoning was also found to be completely reversible and the catalyst immediately regained its initial activity when the sulphur was removed from the feed [4]. Furthermore, under the typical operating conditions of methane CPO, i.e. at high temperatures (>800 °C) and short contact times, the sulphur storage capacity of the support did

not show any beneficial effect on the sulphur tolerance of the catalyst [4]. Contrary to what was observed when the CPO of methane was carried out in the low- to moderate-temperature regime (300–800 °C), where nature of the support material played a crucial role in the partial oxidation reaction [5].

Many studies have been published on the partial oxidation of methane over noble metals but only few studies have been done very recently in the presence of sulphur compounds [3,6]. Although there has been no direct study on the improvement on the sulphur tolerance of Rh-based catalysts conducted under CPO conditions, it has been reported that the addition of Pt [7] or Pd [8] to Rh improves the activity of the catalyst during the steam reforming of sulphur-containing fuels. In addition the partial substitution of Rh with Pt or Pd will be highly economical due to high cost of Rh metal. Accordingly, the purpose of this work is to investigate the enhancement in sulphur tolerance of Rh-based catalyst by partially substituting Rh with either Pt or Pd under self-sustained steady state operation at high temperatures and short contact times as well as during low-temperature light-off phase. This work uses in situ diffuse reflectance infrared Fourier transform (DRIFT) spectroscopy of adsorbed CO at room temperature to investigate changes on the surface state of rhodium before and after exposure to sulphur species at temperatures and conditions close to those expected under actual CPO of methane. Furthermore, an attempt is made to identify sites responsible for

* Corresponding author at: Istituto Ricerche sulla Combustione, CNR, P.le V. Tecchio 80, 80125 Napoli, Italy. Tel.: +39 081 7682233; fax: +39 081 5936936.

E-mail address: stefano.cimino@cnr.it (S. Cimino).

the loss in the catalytic activity by comparing the results with the activity data.

2. Experimental

2.1. Catalyst preparation

Commercial honeycomb monoliths with straight and parallel channels of roughly square section (cordierite, 600 cpsi by NGK) were cut in the shape of disks of 17 mm diameter and 10 mm long and washcoated with 3% La₂O₃-stabilised γ -Al₂O₃ (SCFa140-L3 Sasol) by a modified dip-coating procedure [2,4]. Monometallic Rh catalysts were prepared via incipient wetness impregnation onto washcoated monoliths using an aqueous solution of Rh(NO₃)₃ (Aldrich) to achieve the desired loading of ~1.0% (w/w). After impregnation, the catalysts were dried at 120 °C and calcined in air at 550 °C. Bimetallic Rh–Pt and Rh–Pd catalysts were prepared by sequentially impregnating calcined Rh (loading 0.5 wt.%) monolith samples with a solution of H₂PtCl₆ or Pd(NO₃)₂. The target Rh/Pt and Rh/Pd weight ratio was 1 with a total metal loading of 1.0 wt.%. Reference powder catalysts with same composition were prepared by incipient wetness impregnations of the γ -Al₂O₃ powders used as washcoat for the monoliths. Furthermore a 1.0 wt.% Rh supported on α -Al₂O₃ powder was also prepared by the same procedure. All the catalysts were calcined in air at 550 °C for 3 h.

2.2. Catalyst characterization

Actual metal content was quantitatively determined on selected fresh and used catalysts by inductively coupled plasma spectrometry (ICP) on an Agilent 7500 ICP-MS instrument, after the microwave-assisted digestion of samples in nitric/hydrochloric acid solution.

BET specific surface area of samples was evaluated by N₂ adsorption at 77 K using a Quantachrom Autosorb 1-C which was also used for CO chemisorptions experiments. Prior to CO adsorption measurement, the sample was heated under He at 120 °C for 30 min and then at 800 °C under a flow of pure H₂. After 1 h at this temperature, the sample was evacuated and cooled under vacuum to 40 °C where CO adsorption was performed.

Temperature programmed desorption (TPD) experiments were performed to examine the extent of catalyst sulphation. The sample, typically 0.1 g (300–400 μ m), was placed in a fixed bed quartz flow reactor and its temperature was monitored by a K-type thermocouple embedded in the catalytic bed. Prior to the TPD measurements, the catalysts were sulphated *in situ* by flowing 80 ppm SO₂ in air at 300 °C for 1 h, during which the samples were exposed to approximately 23 mg S/g of catalyst. Following sulphur poisoning, the sample was heated from 300 to 1000 °C in a stream of N₂ (20 L min^{−1}) at 10 °C min^{−1} and the evolution of SO₂ was monitored by an on-line SO₂/H₂S continuous gas analyser (ABB AO2020 series).

The nature of metal species was investigated by DRIFT spectroscopy using CO as a probe molecule. DRIFT experiments were performed on a Perkin Elmer Spectrum GX spectrometer with a spectral resolution of 4 cm^{−1} and averaged over 50 scans. For each experiment approximately 0.03 g of finely ground powder sample was placed into the ceramic cup of a commercial high-temperature Pike DRIFT cell equipped with a ZnSe window and connected to mass-flow controlled gas lines. The sample was then treated in the following way: (i) prior to the experiments the sample was reduced with a 2% H₂/N₂ mixture for 1 h at 800 °C and then cooled down to room temperature under the same mixture. The sample was purged with Ar for about 15 min before a

background spectrum was recorded; (ii) CO was adsorbed at room temperature (2% CO/N₂ mixture, 100 cm³ min^{−1}) for 30 min and any excess CO was removed by flushing with Ar (100 cm³ min^{−1}) prior to recording the IR spectra; (iii) the sample was then flushed with Ar at 800 °C for 15 min followed by exposure to 20 ppm H₂S/2% H₂-N₂ (100 cm³ min^{−1}) mixture for 30 min; (iv) after sulphation at 800 °C, the sample was cooled down to room temperature under the same reaction mixture followed by purging with Ar for approximately 15 min before CO adsorption. All spectra were ratioed against the background spectra collected on the adsorbate-free sample at room temperature. The effect of the regeneration of S-poisoned catalyst by reduction under a mixture of 2% H₂/N₂ at high temperatures was also investigated.

2.3. Catalyst testing

The catalytic honeycombs were stacked between two mullite foam monoliths (45 ppi, *L* = 12 mm) as heat shields and placed in a quartz tube inserted in an electric furnace that was used for pre-heating the feed mixture. Reactor temperatures were measured by means of K-type thermocouples (*d* = 0.5 mm) placed in the middle of the central channel of the catalyst, in close contact with the solid, as well as in the gas upstream and downstream of heat shields. Further details on the experimental set up were already reported elsewhere [2,4].

High-purity gases (CH₄, O₂, N₂, H₂S 206 ppm in N₂ and SO₂ 185 ppm in N₂) calibrated via 5 Brooks 5850-series mass-flow controllers were pre-mixed and fed to the reactor at gas hourly space velocity (GHSV) comprised between 5 and 8 × 10⁴ h^{−1} (standard conditions and based on the volume of the catalytic honeycomb) corresponding to residence times as low as 14 ms at the average reactor temperature of 900 °C. Methane catalytic partial oxidation tests were run under self-sustained pseudo-adiabatic conditions at fixed pre-heating (250 °C) and an overall pressure of *P* = 1.2 bar, either using simulated air as oxidant, or oxygen with N₂ added to obtain a fixed dilution level (10 or 20 vol.%) of the feed. The catalytic monoliths were tested after stabilisation upon exposure to standard reacting conditions. The impact of sulphur addition on the catalytic performance was studied at CH₄/O₂ feed ratios in the range 1.6–2 under both transient and steady state conditions. The sulphur level was varied between 2 and 58 ppm on a molar basis with respect to the total flow of gases by partially substituting the N₂ flow in the feed with an equal flow of H₂S in N₂ mixture.

Catalytic light-off temperatures were determined by ramping-up the external furnace from 200 °C to the light-off temperature at a rate of ~5 °C/min under transient conditions using methane–air mixtures at fixed feed ratio (CH₄/O₂ = 1.8), in the absence and presence of 20 ppm H₂S.

Methane conversion, yields and selectivities to CO and H₂ were calculated according to the definitions:

$$x_{\text{CH}_4} = 100 \times \left(1 - \frac{\text{CH}_4^{\text{OUT}}}{\text{CH}_4^{\text{OUT}} + \text{CO}_2^{\text{OUT}} + \text{CO}^{\text{OUT}}} \right)$$

$$Y_{\text{CO}} = 100 \times \left(\frac{\text{CO}^{\text{OUT}}}{\text{CH}_4^{\text{OUT}} + \text{CO}_2^{\text{OUT}} + \text{CO}^{\text{OUT}}} \right), \quad S_{\text{CO}} = 100 \times \left(\frac{Y_{\text{CO}}}{x_{\text{CH}_4}} \right)$$

$$Y_{\text{H}_2} = \frac{100}{2} \times \left(\frac{\text{H}_2^{\text{OUT}}}{\text{CH}_4^{\text{OUT}} + \text{CO}_2^{\text{OUT}} + \text{CO}^{\text{OUT}}} \right), \quad S_{\text{H}_2} = 100 \times 2 \times \left(\frac{Y_{\text{H}_2}}{x_{\text{CH}_4}} \right)$$

based on the exit dry-gas mol fractions of CO, CO₂, CH₄ and H₂ independently measured by a continuous analyser with cross

Table 1

BET, ICP-MS and CO chemisorptions for structured catalysts and their corresponding supports.

Sample	Honeycomb ^a <i>L × d</i> (mm)	Washcoat material	B.E.T. ^b (m ² /g)	ICP ^b (wt.%)			CO monolayer ^c (mmol/g pgm)	Dispersion ^c (%)
				Rh	Pt	Pd		
AA	–	α-Al ₂ O ₃	7.8	–	–	–	–	–
LA	–	3% La ₂ O ₃ –γ-Al ₂ O ₃	143	–	–	–	–	–
Rh/AA	–	–	8.0	0.92	–	–	0.90	6.7
Rh/LA	10 × 17	LA	150	0.95	–	–	5.54	42
Rh–Pt/LA	10 × 17	LA	151	0.50	0.48	–	3.53	–
Rh–Pd/LA	10 × 17	LA	153	0.51	–	0.60	3.60	–

^a Cordierite, 600 cpsi, channel side 0.96 mm, wall thickness 76 μm.^b Referred to total weight of active phase, monolith substrate excluded.^c By CO chemisorptions after reduction in H₂ at 800 °C; CO/Rh = 1.

sensitivity correction (ABB Advance Optima). No other hydrocarbons except from methane were detected in the products, whereas O₂ was always completely converted under steady state operation (TCD–GC analysis) after light-off had occurred; H₂O production was calculated from the O-balance. Carbon and hydrogen balances were always closed within ±1.5% and ±3.5%, respectively. Sulphur species were not directly measured but preliminary TGA analysis excluded any significant sulphur capture effect by materials placed in the reactor before the catalyst (i.e. mullite and SiC foams) under representative operating conditions.

3. Results and discussion

3.1. Characterization

Table 1 illustrates catalyst denomination, total surface areas and their total CO uptake after H₂ reduction at 800 °C. The commercial γ-alumina stabilised with La₂O₃ is characterized by a specific surface area of ~140 m²/g in contrast to 8 m²/g of the α-alumina employed to prepare reference Rh catalyst for DRIFT experiments: as a result the Rh/AA sample has a much lower CO uptake and metal dispersion with respect to the Rh/LA sample. The metal dispersions were calculated by assuming the stoichiometric factor between the CO and metal atoms to be 1:1. However, since the stoichiometric ratio depends on the precious metal and several possible forms of adsorbed CO may coexist, caution should be exercised when comparing the dispersion values of different catalysts.

In particular, CO adsorption on Rh changes from predominantly linear to gem-dicarbonyl form for catalysts with low and high rhodium dispersion, respectively [9,10] (see DRIFT experiments). In addition, since CO can adsorb on Rh, Pt and Pd, it is not possible to measure the number of each metal sites independently, consequently the chemisorptions data are also reported in terms of the total amount of CO for monolayer coverage per gram of precious metal. The Rh/LA sample has the highest CO uptake, due to its high Rh content and large surface area of the support material. The bimetallic catalysts have similar CO uptake due to the substitution of half of Rh for Pt or Pd.

The actual loadings of noble metals (Table 1) are close to the nominal one for all catalysts: in particular it can be noticed that Rh content is halved in bimetallic samples and substituted by a corresponding weight of Pt or Pd. BET values for the final monolith catalysts after the deposition of precious metals are in line with the corresponding support washcoat layer (~150 m²/g), which was obtained with the addition of alumina binder and calcination in air at 800 °C.

SEM inspection of all monoliths showed a good adhesion of the washcoat whose accumulation in the corners causes the typical rounding of the originally squared channels of the cordierite substrate. SEM/EDS mapping on both longitudinal and transverse

sections of the monoliths indicated that the sequential impregnation procedure employed for the preparation of bimetallic systems ensured a uniform dispersion of precious metals throughout the washcoat layer (but not in the cordierite support): this is shown in Fig. 1 by the EDS maps in false colours for Rh and Pt.

DRIFT spectra of adsorbed CO on pre-reduced catalysts provide information on the state and morphology of the Rh component as the adsorption mode of CO is sensitive to different rhodium structures [8]. In order to gain insight into the nature of the Rh active sites during the CPO of methane in the absence and presence of sulphur under self-sustained reaction conditions at high temperatures, DRIFT experiments were carried out at room temperature before and after the sulphation of the sample at 800 °C under H₂S/H₂ reaction mixture. The reducing nature of the sulphur-containing mixture was chosen in order to realize conditions close to those prevailing during actual autothermal operation, since both short contact time and high reactants concentration used in the catalytic tests could not be reproduced in the DRIFT cell. Furthermore, preliminary tests indicated that the effect of sulphur poisoning was independent from the type of sulphur precursor (SO₂ or H₂S) in the presence of high concentrations of H₂.

The dominant features of the DRIFT spectrum of CO adsorbed over reduced Rh/LA (Fig. 2a) are the doublet bands at 2090 and 2016 cm^{−1} corresponding to gem-dicarbonyl species on isolated Rh atoms. The presence of these bands is related to highly dispersed Rh metal particles on the catalyst surface [10]. However, there is also a presence of a very weak band at around 2060 cm^{−1} which can be assigned to the linearly adsorbed CO on Rh

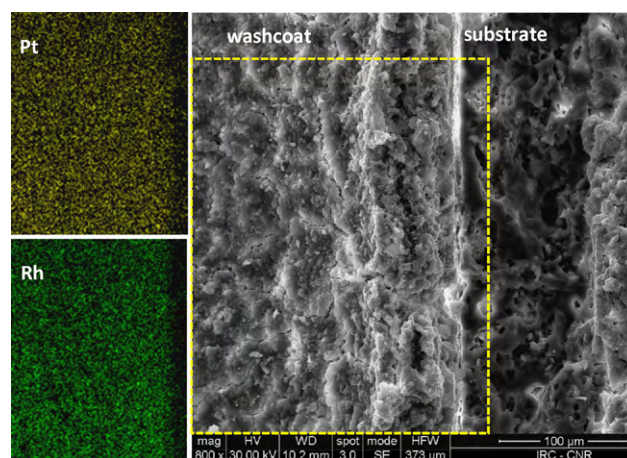


Fig. 1. SEM image of a longitudinal section of the Rh–Pt bimetallic monolith catalyst with corresponding false colours EDS maps showing Pt and Rh distribution in the stabilised alumina washcoat layer (LA). (For interpretation of the references to colour in this figure legend, the reader is referred to the web version of the article.)

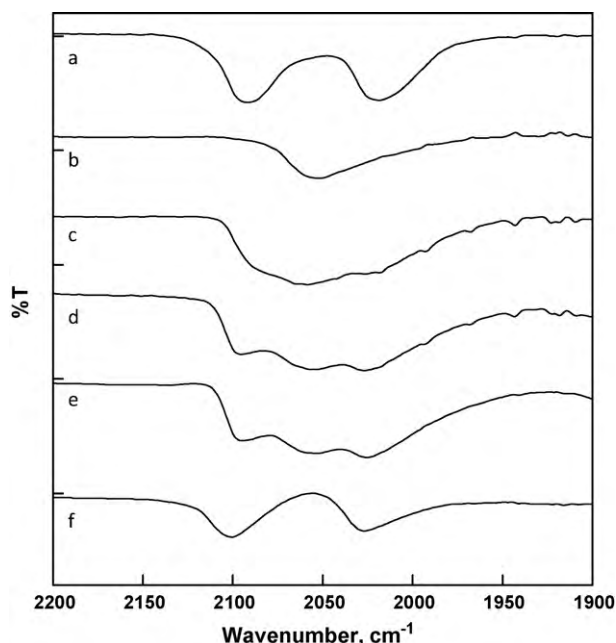


Fig. 2. DRIFT spectra of CO adsorption at room temperature over Rh/LA catalyst following: (a) reduction of fresh catalyst at 800 °C for 1 h, (b) H₂S/H₂ reaction at 800 °C for 30 min, (c) regeneration under 2% H₂-N₂ reaction mixture for 1 h at (c) 500 °C, (d) 600 °C, (e) 700 °C and (f) 800 °C. Spectra are offset for clarity.

crystallites or clusters in the zero oxidation state, the identification of which is impeded by the overlap with the twin dicarbonyl bands. The presence of linear and dicarbonyl features in the spectrum indicates the existence of two different adsorption sites on the surface of the catalyst. Following the sulphation of the sample at 800 °C and cooling down under H₂S/H₂ reaction mixture, the band at 2060 cm⁻¹ becomes the only distinct band in the CO spectrum indicating the presence of only linearly adsorbed CO – Fig. 2b. These results suggest that only the dispersed Rh species (responsible for Rh-(CO)₂ formation) are affected by S-poisoning while the Rh-CO species are not modified by sulphur. Thus, sulphur appears to act as a selective poison which preferentially adsorbs on smaller crystallites, i.e. sulphur adsorption on Rh is structure-sensitive [11]. Fig. 2c–e illustrates the effect of catalyst regeneration by reduction at progressively higher temperatures (500–700 °C) which results in an increase in the intensity of the doublet bands. Reduction at 800 °C results in the complete reappearance of the gem-dicarbonyl bands illustrating that the sulphur poisoning is reversible – Fig. 2f.

In order to confirm the selective adsorption of sulphur on highly dispersed Rh sites, the same experiments were repeated on Rh/AA catalyst with a lower precious metal dispersion (Table 1), due to the much lower surface area of α -Al₂O₃ support. Accordingly, the DRIFT spectrum of the CO adsorbed at room temperature over reduced Rh/AA sample reveals a strong band at 2070 cm⁻¹ and two shoulders at 2098 and 2025 cm⁻¹ as shown in Fig. 3a. The fact that absorption bands of the dicarbonyl species were poorly developed and the band ascribable to linear CO was much more intense confirms a higher fraction of larger metallic Rh particles with respect to the highly dispersed Rh⁺ phase. This result is in agreement with the latest findings on Rh/ α -Al₂O₃ where increasing Rh concentration in the sample resulted in an increase in the intensity of the linear CO band due to growth in metal particle size [12]. The difference in the position of the linear CO bands on freshly reduced rhodium sites on La- γ -Al₂O₃ (2060 cm⁻¹) and α -Al₂O₃ (2070 cm⁻¹) is a consequence of different particle size. This result agrees with the observation that frequencies of CO species shift to

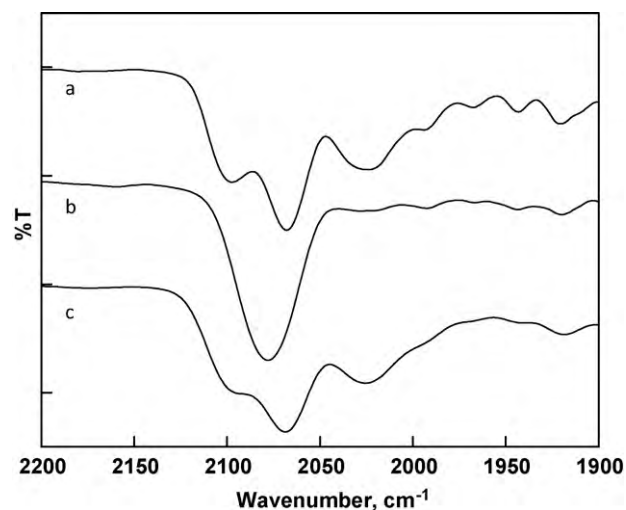


Fig. 3. DRIFT spectra of CO adsorption at room temperature over Rh/ α -Al₂O₃ following: (a) reduction of fresh catalyst at 800 °C for 1 h; (b) H₂S/H₂ reaction at 800 °C for 30 min and (c) after hydrogen reactivation at 800 °C for 1 h.

higher wavenumbers for bigger metal particles [13]. After H₂S/H₂ reaction mixture at 800 °C for 30 min the band at 2070 cm⁻¹ becomes the only distinct band in the CO spectrum (Fig. 3b) with the gem-dicarbonyl species being completely removed from the rhodium surface, exemplifying the preferential adsorption of S on isolated Rh⁺ sites. However, the IR band due to adsorbed linear CO is found to shift slightly to higher wavenumbers (from 2070 to 2080 cm⁻¹) following sulphation. The upward shift in the vibrational frequency is likely to be due to the increase in the dipole–dipole coupling as a result of a higher coverage of adsorbed CO. A similar behaviour is also reported by Anderson et al. [14] who observed that the evacuation of CO at room temperature and at higher temperatures caused the strong band at 2071 cm⁻¹, attributed to linearly adsorbed CO shift to 2058 cm⁻¹, due to a decrease in dipole coupling between adjacent CO molecules. In an attempt to reactivate the sulphur-poisoned catalyst, the sample was treated with hydrogen at 800 °C for 1 h. The relative intensity of the peak at 2080 cm⁻¹ decreased and at the same time returned back to its initial wavenumber (2070 cm⁻¹), while the intensities of the gem-dicarbonyl bands increased, indicating that the catalyst can be regenerated by hydrogen treatment. In conclusion, the above IR measurements confirm that sulphur preferentially adsorbs on smaller Rh crystallites which are much less abundant on Rh/AA catalyst where the formation of large metallic particles (Rh⁰) is favoured.

Fig. 4 shows the IR spectra of CO adsorbed at room temperature on the reduced, sulphur-poisoned and hydrogen-reactivated Rh-Pt/LA catalyst. Once again the spectrum is dominated by bands at 2095 and 2025 cm⁻¹ due to a rhodium gem-dicarbonyl species following sample reduction at 800 °C, as shown in Fig. 4a. However, the presence of a shoulder at 2060 cm⁻¹ which was masked by the intense dicarbonyl bands for supported rhodium only, is clearly visible for the bimetallic catalyst. It has been stated by many authors [15–17] that CO adsorption on Pt gives two bands attributed to linear (2050–2070 cm⁻¹) and bridge forms (1840–1860 cm⁻¹) although Chang and Chang [18] observed only one peak at 2060 cm⁻¹ following CO adsorption over fresh Pt/ γ -Al₂O₃ catalyst. In our experiments the band at 1845 cm⁻¹ was very weak and in some cases it was not detected. The band at 2060 cm⁻¹ can be assigned to CO adsorption on Pt clusters which also includes to a lesser extent the contribution of CO bonded to metallic Rh particles. The infrared absorption bands of the CO adsorbed at room temperature following exposure to H₂S is shown in Fig. 4b.

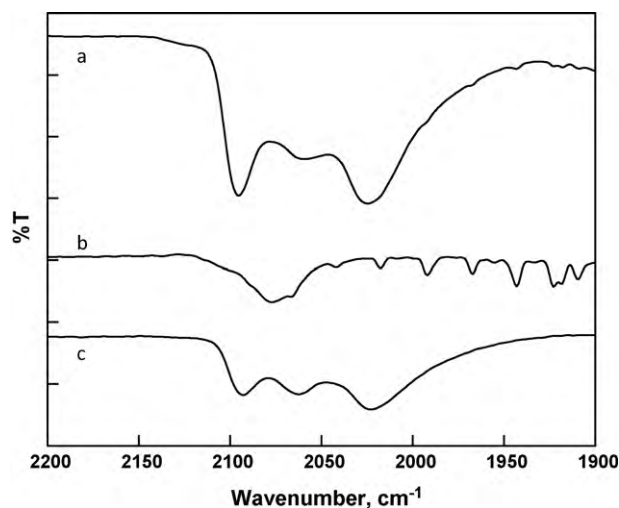


Fig. 4. DRIFT spectra of CO adsorption at room temperature over Rh–Pt/La–Al₂O₃ catalyst following: (a) reduction of fresh catalyst at 800 °C for 1 h; (b) H₂S/H₂ reaction at 800 °C for 30 min and (c) hydrogen reactivation at 800 °C for 1 h.

Once again the linearly adsorbed CO band becomes the only distinct band in the CO spectrum following sulphation accompanied by a shift to higher wavenumbers, from 2060 cm^{−1} for a freshly reduced sample to 2075 cm^{−1} following sulphation. The shift to higher frequency is consistent with the IR spectra characterizing CO adsorbed on sulphur-poisoned Pt catalysts, reported by Hoyos et al. [19] and is suggested to be a consequence of the partial deposition of sulphur on Pt clusters, and/or the formation of PtS. Following hydrogen treatment (Fig. 4c) the spectrum of the hydrogen-reactivated sample, although the bands are less intense compared to the freshly reduced sample, the profile of the spectra are very similar, suggesting that also the bimetallic Rh–Pt catalyst can be reactivated following sulphur poisoning.

Fig. 5 illustrates the infrared spectra of CO adsorbed at room temperature on Rh–Pd/LA catalyst. Following sample reduction (Fig. 5a), the only bands observed (2090 and 2017 cm^{−1}) are due to the gem-dicarbonyl CO species formed on well-dispersed rhodium particles. These bands are overlapped with the very weak IR band of the linear species (~2060 cm^{−1}). It has to be noted, however,

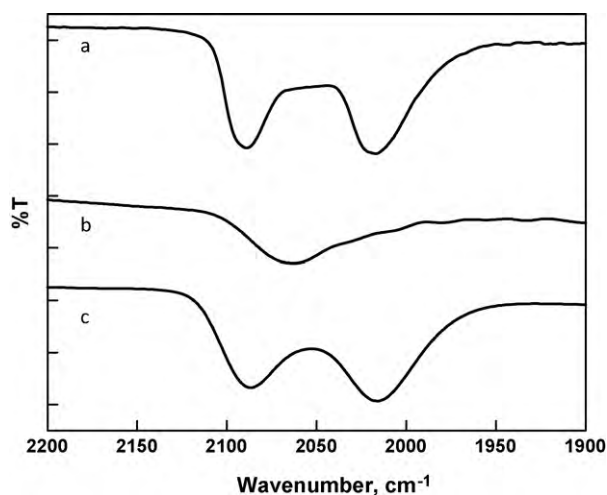


Fig. 5. DRIFT spectra of adsorbed CO on Rh–Pd/La–Al₂O₃ catalyst at room temperature after: (a) reduction of fresh catalyst at 800 °C for 1 h; (b) H₂S/H₂ reaction at 800 °C for 30 min and (c) hydrogen regeneration at 800 °C for 1 h.

that unlike the bimetallic Rh–Pt catalyst (Fig. 4a), which clearly exhibited the band corresponding to linear adsorbed CO (at 2060 cm^{−1}) on metallic Pt particles, the band typically attributed to linear adsorbed CO on Pd (at 2060–2070 cm^{−1}) [20,21] in the Rh–Pd sample is absent. It has also been reported that the intensity of bands related to linear CO adsorbed on rhodium is more intense than the corresponding bands on Pd [21]. Moreover, the linear CO band on palladium is strongly affected by reduction cycles [20] or even by evacuation treatment at room temperature [21], thus in these spectra the contribution of the Pd⁰–CO species can be tentatively neglected. Furthermore, it has been shown that under oxidising conditions, the Pd–Rh alloys were enriched in palladium, whereas under reducing condition, palladium particles tend to segregate while rhodium could diffuse through the Pd layer without any phase separation of the alloy particles [22,23]. The reason that the spectrum of CO adsorbed on freshly reduced Rh–Pd sample is characteristic of well-dispersed Rh particles, could be due to the presence of palladium which promotes the formation of Rh gem-dicarbonyl species. Similar conclusion was also reached by Maillet et al. [21] following the reduction treatment of various alumina supported Pd–Rh catalysts at high temperatures. After treatment in the H₂S/H₂ reaction mixture at 800 °C, the spectrum of CO adsorbed at room temperature (Fig. 5b) is characteristic of linear CO–Rh⁰ species (band at 2060 cm^{−1}) as observed on Rh only catalyst, with the complete removal of the gem-dicarbonyl species. Regeneration at 800 °C in the reducing atmosphere results in the reappearance of the gem-dicarbonyl bands illustrating that the sulphur poisoning is reversible – Fig. 5c.

Overall, the above DRIFT studies indicate that the addition of another noble metal such as Pt or Pd does not influence directly the way sulphur adsorbs and interacts on the highly dispersed Rh sites.

3.2. CPO light-off

It has already been demonstrated that the presence of sulphur in the reaction feed on Rh-based catalysts shifts the minimum catalyst light-off for CPO to higher temperatures [4]. The shift in the catalyst light-off temperature is due to sulphur poisoning which reduces the availability of active metal sites. During the transient pre-ignition period the catalyst is exposed to a large partial pressure of oxygen. Table 2 illustrates the effect of the addition of 20 ppm H₂S in the reaction feed on the ignition of methane–air mixtures at fixed feed ratio (CH₄/O₂ = 1.8) over LA supported Rh, Rh–Pt and Rh–Pd monolith samples pre-reduced under reaction conditions: the results are presented in terms of both minimum light-off temperatures and final operating temperature under self-sustained operation at fixed pre-heating. It can be seen that both in the absence and in the presence of sulphur, the monometallic Rh sample which has the highest Rh content shows the lowest light-off temperature (270 and 302 °C, respectively), indicating that the dissociation of methane occurs more readily over Rh active sites under the studied reaction condition. In fact the substitution of half of the Rh loading with either Pt or Pd causes a

Table 2

Effect of H₂S addition on light-off and on the final catalyst temperature during CPO of methane under self-sustained operation at pre-heating temperature of 350 °C (T_{cat}) over La–Al₂O₃ supported Rh, Rh–Pt and Rh–Pd monoliths. CH₄/O₂ = 1.8 in air, GHSV = 8 × 10⁴ h^{−1}.

Catalyst	H ₂ S = 0 ppm		H ₂ S = 20 ppm		ΔT light-off (°C)	ΔT_{cat} (°C)
	Light-off (°C)	T _{cat} (°C)	Light-off (°C)	T _{cat} (°C)		
Rh	270	750	302	909	32	159
Rh–Pt	290	816	309	900	19	84
Rh–Pd	289	770	333	942	44	172

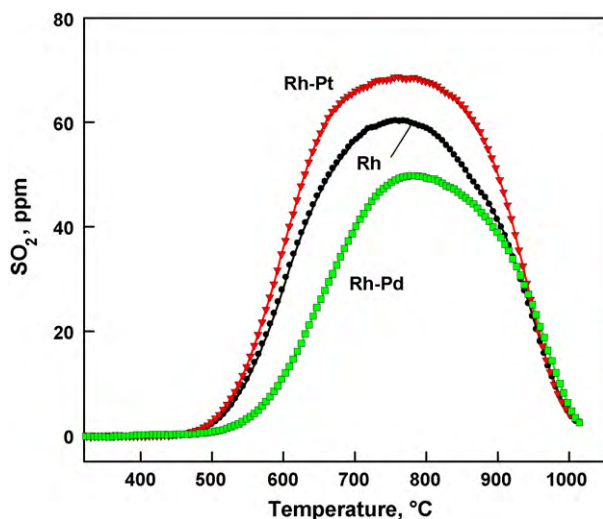


Fig. 6. TPD profiles of SO_2 from S-aged Rh, Rh–Pt and Rh–Pd supported (LA) catalysts (300°C , 100 ppm SO_2 in air, 2 h ~ 14 mg of S/g_{cat}).

rise of the minimum light-off temperature to about 290°C regardless of the nature of the second precious metal. It should be noted however that, the increase in the catalyst light-off temperature and in the catalyst operating temperature, observed for all the catalysts before and after the addition of H_2S in the feed, is smallest over the bimetallic Rh–Pt catalyst and largest over the Rh–Pd sample (Table 2). Therefore, Pt appears able to limit the poisoning effect of sulphur towards Rh sites, whereas the opposite trend is observed in the presence of Pd.

In order to get further insights on the reason for such protecting effect, TPD experiments were carried out following S ageing of the three supported Rh, Rh–Pt and Rh–Pd catalysts at 300°C with 100 ppm SO_2 in air for 2 h. Results are shown in Fig. 6 comparing desorption profiles of SO_2 which was the only detected S-species. All the catalysts show a broad desorption peak centered at $750\text{--}780^\circ\text{C}$ which appears to be mostly due to the decomposition of very stable aluminum sulphate species [5]. The possible contribution of other S-species is masked by the main signal. From the peak areas the amount of sulphur taken up by the catalysts decreases in the order Rh–Pt > Rh > Rh–Pd (0.95, 0.79 and 0.60 mg of S/g_{cat} , respectively). The higher amount of S uptake on the bimetallic Rh–Pt catalysts corresponds to the higher oxidation activity of Pt which more readily oxidises SO_2 to SO_3 rather than Rh and Pd [24]. Once oxidised to SO_3 the sulphur species can be readily stored on

the catalyst support as $\text{Al}_2(\text{SO}_4)_3$ thus minimising the build-up of S on or close to the active Rh sites where methane activation reactions take place. On the other hand the detrimental effect of Pd in the bimetallic Rh–Pd system is due to its higher sensitivity to sulphur poisoning and the formation of stable PdSO_4 species [24]. This reduces the rate of SO_3 formation and SO_3 migration on to the support which in turn decreases the sulphation of the support material while leading to the higher accumulation of sulphate species around the precious metal which inhibits the catalytic activity. In analogy to the current results, it was already reported that the use of a less sulphating support for Rh such as a $\text{SiO}_2\text{--Al}_2\text{O}_3$ does not enhance the sulphur tolerance of the catalyst with regards to light-off delay, since more sulphur tends to stick close to the Rh active sites [5].

3.3. CPO activity measurement

Fig. 7 compares the catalytic activities of LA supported Rh, Rh–Pt and Rh–Pd catalysts during the CPO of methane, under pseudo-adiabatic conditions at a fixed CH_4/O_2 feed ratio, using 10% N_2 dilution, in the absence or presence of 20 ppm H_2S .

In the absence of sulphur monometallic Rh catalyst showed the best performance in terms of methane conversion and CO and H_2 yields. Substitution of half of the Rh loading with same weight amount of Pt and even more with Pd entails a reduction in fuel conversion and yield to syngas. This is accompanied by a significant increase in the operating temperatures measured on bimetallic monoliths. Among bimetallic catalysts, Rh–Pt performs better than Rh–Pd. Such results confirm that Rh is the most active and selective metal for methane CPO, whereas on both Pt and Pd reactions leading to total oxidation products become more important. In fact it was reported that the higher syngas yield on Rh is strictly associated to its higher methane steam reforming activity whose contribution is significant even at very short contact times [25].

The presence of 20 ppm H_2S in the reaction feed resulted in a loss in the activities and an increase in the surface temperature by $\geq 100^\circ\text{C}$ of all the catalysts, the effect being more pronounced over the Rh–Pd system. The decrease in methane conversions in the presence of sulphur was accompanied by a decrease in CO yield of similar magnitude (except for Rh–Pt) while in comparison the drop in H_2 yield was always larger. The decrease in the catalytic performances and the rise in the catalyst temperature in the presence of H_2S is an indication of the inhibition of the steam reforming reaction, as shown in previous studies [3,4]. The significant loss in activity observed over the Rh–Pd catalyst could be caused by the formation of stable palladium sulphide or due to

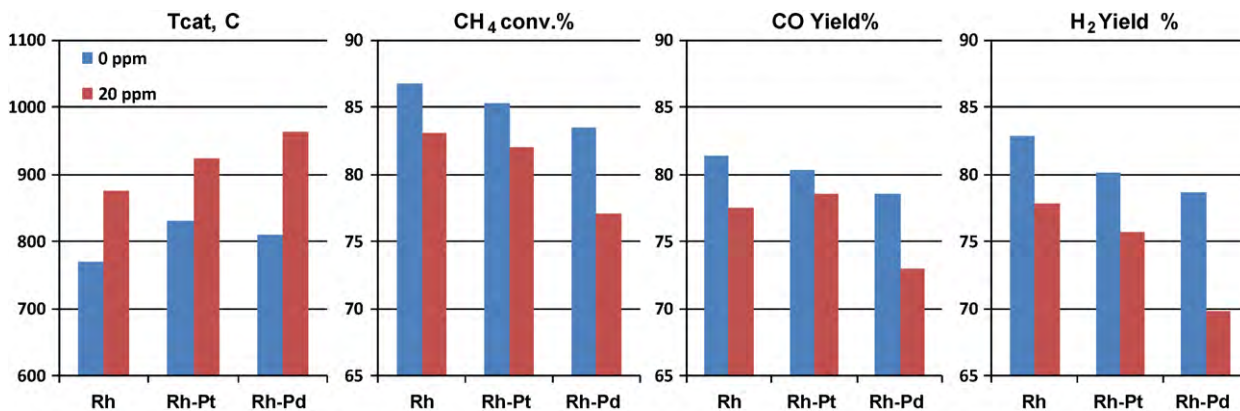


Fig. 7. Comparison of CH_4 conversion, CO and H_2 yield and catalyst temperature on Rh, Rh–Pt and Rh–Pd supported on $\text{La-Al}_2\text{O}_3$ catalysts in the absence and presence of 20 ppm H_2S . $\text{CH}_4/\text{O}_2 = 2$, GHSV = $6.1 \times 10^4 \text{ h}^{-1}$ and $\text{N}_2 = 10 \text{ vol.}\%$.

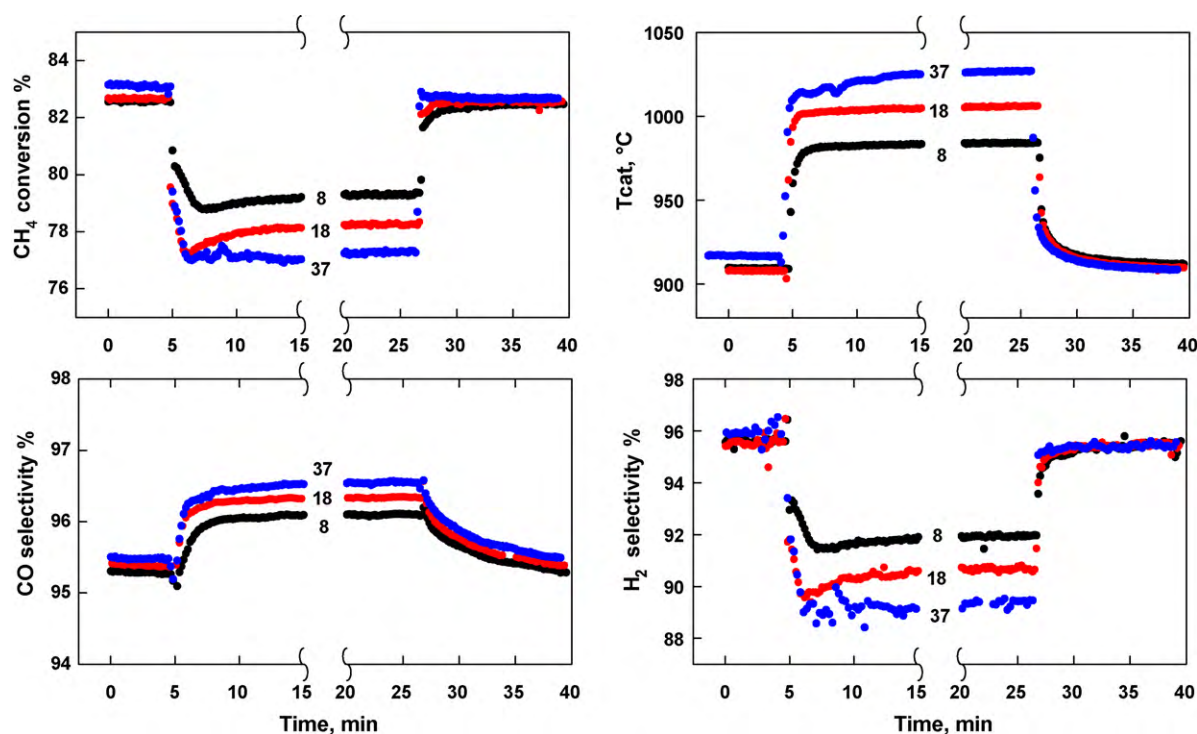


Fig. 8. Transient response to H₂S addition (8, 18 or 37 ppm) and removal on methane conversion, catalyst temperature, CO and H₂ selectivities during methane CPO on Rh–Pt/LA monolith. Feed CH₄/O₂ = 2, GHSV = $6.7 \times 10^4 \text{ h}^{-1}$, N₂ = 20 vol.%.

the migration of sulphur into bulk Pd which can then adversely affect the Rh–Pd interaction. An alternative explanation may be due to the presence of highly dispersed Rh particles on the surface of the Pd particles, which are more readily poisoned by the sulphur in the reaction feed, since it was shown in Section 3.1 (Fig. 5) that the presence of palladium promotes the formation of Rh gem-dicarbonyl species. These results also support our previous findings [4] where the inhibition effect of S was found to be greater over a sample which had higher Rh dispersion.

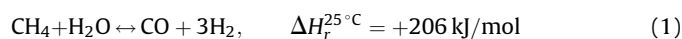
Unlike the Rh–Pd system, however, the bimetallic Rh–Pt catalyst with only half the amount of rhodium content by weight (2:1 Rh:Pt molar ratio) showed a better specific tolerance to sulphur inhibition since the overall catalytic performance is close to the monometallic Rh catalyst. As a result, further studies were carried out over the bimetallic Rh–Pt catalyst in order to gain better understanding of its improved performance.

Fig. 8 illustrates the transient effect of addition and removal of 8, 18 and 37 ppm H₂S to and from the reaction mixture under CPO conditions over Rh–Pt/LA monolith operated at a fixed CH₄/O₂ feed ratio, using 20% N₂ dilution. The addition of H₂S resulted in a sharp decrease in CH₄ conversion and H₂ selectivity with a corresponding rapid increase in the catalyst temperature following a similar trend to that observed in our previous study over the monometallic Rh/LA monolith [4]. However, unlike the monometallic Rh sample where the CO selectivity was almost unaffected, even at the highest sulphur concentrations [4], there is a slight increase in the CO selectivity over the bimetallic Rh–Pt which increases with H₂S concentration in the feed. The extent of reaction inhibition by S was also found to be greater at lower H₂S concentration. However, the inhibition effect of sulphur did not reach a saturation level even at H₂S concentrations of 37 ppm.

Upon removing the H₂S from the reaction feed, the initial conversion and product distribution were regained immediately. The recovery in the catalytic activity was also accompanied by a sharp decrease in the catalyst temperature to its initial value before the H₂S addition, indicating that the sulphur poisoning

effect was completely reversible under the studied reaction condition, in accordance with the above DRIFT studies. Furthermore, the rapid response upon the introduction and removal of sulphur suggests that the inhibition was caused by selective reversible sulphur adsorption onto the metal active sites. However, as seen in Fig. 8 the catalyst performance continues stable in the presence of H₂S indicating that there is a steady state between S adsorbing on the surface of the active sites and S desorbing into the gas phase, which is governed by the catalyst temperature and sulphur concentration.

The differences in the catalytic CPO performance of Rh–Pt/LA monolith at steady state due to increasing H₂S concentrations at a fixed CH₄/O₂ feed ratio are summarized in Table 3. It can be seen that the reduction in methane conversion (ΔCH_4) following sulphur addition is accompanied by a larger reduction in hydrogen production (ΔH_2), with a molar ratio ($\Delta\text{H}_2/\Delta\text{CH}_4$) of approximately 3.6–3.8. These values are higher than those reported previously for the monometallic Rh catalyst [3,4], which were close to 3, indicating that the poisoning effect of H₂S is related to its ability to inhibit the endothermic steam reforming reaction (Eq. (1)) which mainly occurs in the second region of the catalyst bed, after oxygen has been consumed, between the unconverted methane and water produced in the first oxidation zone of the reactor [25].



In addition, unlike the monometallic Rh catalyst where the decrease in methane conversion in the presence of sulphur was accompanied by a decrease in CO yield of similar magnitude (Fig. 7), over the bimetallic Rh–Pt catalyst CO selectivity rises upon sulphur addition (Fig. 8), and the decrease in CO yield is slightly less than the corresponding reduction in methane conversion.

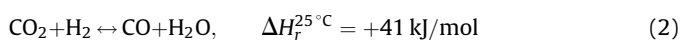
At the same time, unlike the only Rh catalyst [4], the ΔCH_4 does not correspond to the $\Delta\text{H}_2\text{O}$, i.e. the additional amount of water formed in the products is more than what is expected by its missed consumption in methane steam reforming (1). Moreover the

Table 3Effect of H₂S addition at various concentrations on the steady state methane CPO on Rh–Pt/LA monolith. Feed CH₄/O₂ = 2, GHSV = 6.7 × 10⁴ h^{−1}, N₂ = 20 vol.%.

CH ₄ /O ₂ = 2	H ₂ S				Difference ^a		
	0 ppm	8 ppm	18 ppm	37 ppm	Δ (8–0)	Δ (18–0)	Δ (37–0)
x _{CH₄} (%)	82.7	79.3	78.2	77.1	−3.4	−4.5	−5.6
Y _{H₂} (%)	79.0	72.5	71.0	68.8	−13.0	−16.0	−20.4
Y _{CO} (%)	79.0	76.2	75.3	74.4	−2.8	−3.7	−4.6
Y _{H₂O} (%)	3.7	6.8	7.2	8.3	+6.2	+7.0	+9.2
Y _{CO₂} (%)	3.7	3.1	2.9	2.7	−0.6	−0.8	−1.0
H ₂ /CO	2.00	1.90	1.89	1.85			
T _{cat} (°C)	909	984	1005	1025	+75	+96	+116
T _{out} (°C)	696	721	733	744	+25	+37	+48

^a Products molar flows per 100 CH₄ feed.

contribution to H₂O formation and H₂ consumption from the RWGS equilibrium reaction (Eq. (2)), which is favoured at the higher operating temperature attained with sulphur is still not sufficient enough to explain the change in product distribution over Pt–Rh catalyst.



To sum up, products redistribution from the bimetallic Rh–Pt catalyst in the presence of S appears to be the result of two main superimposed effects: (i) inhibition of steam reforming path on Rh sites and (ii) improved process selectivity towards the oxidation of H₂ to H₂O, probably due to the nature of the Pt active sites, which display a higher intrinsic selectivity towards CO and H₂O during methane CPO in comparison to Rh sites [25].

Both effects are compatible with the selective adsorption of S on isolated (well dispersed) Rh sites only. In agreement with the DRIFT results the formation of surface Rh sulphide species does not appear to be directly affected by the simultaneous presence of Pt on the surface of the catalyst. However the equilibrium coverage of Rh by sulphur depends on temperature and partial pressure of H₂ and H₂S, therefore it is indirectly affected by the presence of Pt in the catalyst formulation, since the presence of Pt causes an

increase in the catalyst operating temperature during the self-sustained CPO of methane, due to its higher oxidation activity.

In order to examine the effect of initial catalyst temperature on the extent of sulphur poisoning over the Rh and Rh–Pt catalysts, the CPO reactions were carried out by using N₂ dilutions of either 20 or 55.6 vol.% with the latter corresponding to using air as an oxidant at a fixed CH₄/O₂ feed ratio of 2.

The results are illustrated in Fig. 9 in terms of catalyst temperature, methane conversion, yields to CO and H₂, vs sulphur concentration in the feed.

The temperature profiles for both catalysts display the same increasing trend as sulphur is added, but some major differences can be noted when comparing their behaviours at different dilutions. When using feed conditions with lower N₂ dilution, the bimetallic Rh–Pt system always operates at higher temperatures (~100 °C) than the Rh only sample regardless of the sulphur content in the reaction mixture. Fig. 9 indicates that resulting methane conversions are similar and progressively decrease with S content approaching a plateau above 30 ppm of H₂S.

It can be seen that in the presence of S there is a significant advantage in terms of yield to CO and CH₄ conversion over the Rh–Pt catalyst, whose higher operating temperature appears to be induced by its lower Rh content, thus reducing the impact of S inhibition.

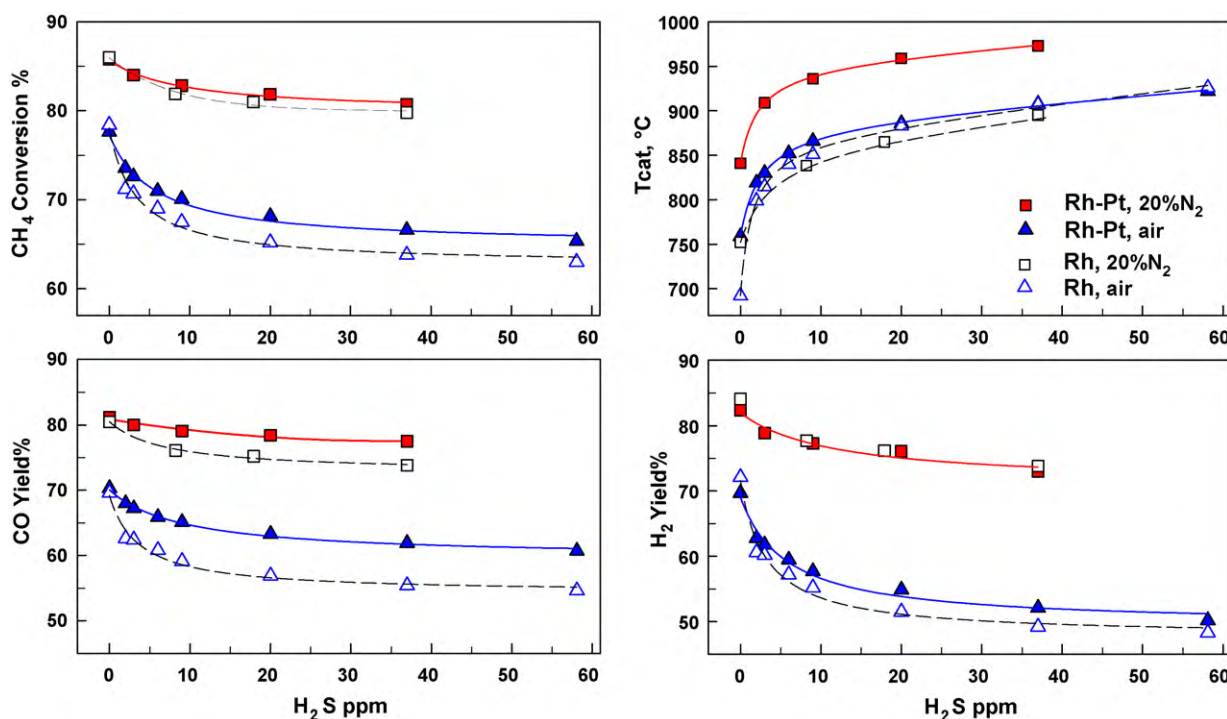


Fig. 9. Effect of H₂S addition on CH₄ conversion yields to CO and H₂ and the catalyst temperature during the CPO of methane over Rh–LA and Rh–Pt/LA monolith at CH₄/O₂ = 2 at two different N₂ dilution levels of the feed (20% and 55.6% = air). GHSV = 6.7 × 10⁴ and 8.1 × 10⁴ h^{−1}, for feed mixture containing N₂ = 20 and 55.6 vol.%, respectively.

It was already shown in Fig. 7 that even at lower dilution ($N_2 = 10\%$), corresponding to higher operating temperature, Rh only catalyst is still able to outperform the bimetallic Rh–Pt counterpart with regards to H_2 yield and methane conversion in the presence of 20 ppm H_2S . When CPO experiments are carried out in air (i.e. at higher dilution), significantly lower methane conversions are achieved over the two catalytic systems, due to the lower contribution from steam reforming associated to the lower operating temperature and shorter contact time. In the absence of sulphur both samples show similar activities in methane conversion and yield to CO while Rh only catalyst forms slightly more H_2 . However, upon the addition of sulphur the rate of the deactivation of Rh–Pt catalyst is slower than its monometallic counterpart, showing higher methane conversions and yields to CO and also H_2 . Furthermore, in the absence of sulphur in the reaction feed, the bimetallic system operates at approximately 70°C higher than its monometallic counterpart while the difference diminishes when adding small amounts of sulphur (2 ppm) to the reaction feed. In the presence of sulphur, the Rh only catalyst shows a bigger jump in the catalyst temperature and a greater loss in CH_4 conversion compared to the Rh–Pt system, thus indicating a higher sensitivity to sulphur poisoning when operating at lower initial reaction temperatures. This was already shown to be related to the equilibrium between formation–decomposition of surface Rh–sulphides species [4].

Therefore the higher sulphur tolerance of the bimetallic catalyst, in particular when operating under dilute reaction environment appears to be strictly connected to both the higher self-sustained catalyst temperatures, which tends to reduce the impact of S on Rh sites favouring surface sulphide decomposition [4], and to the simultaneous presence of Pt sites, whose activity are almost unaffected by S-poisoning. In fact the substitution of some Rh for the less expensive Pt has a similar qualitative effect to the lowering of the feed dilution.

Indeed significant improvement in the sulphur tolerance of the catalyst with increasing reaction temperature has been observed when steam reforming sulphur-containing fuels [27] as the stable S-species decompose more readily at higher reaction temperatures, thus reducing the sulphur coverage on the catalyst surface.

This is a further indication that the presence of Pt in bimetallic Rh–Pt catalyst improves the thermal stability and intrinsic activity of Rh particles for the steam reforming reaction. Similar synergistic effects were also observed by Kaila et al. [7,28] during the autothermal reforming of simulated and commercial low sulphur diesel fuels on bimetallic Rh–Pt catalysts supported on ZrO_2 .

Fig. 10 compares the temperature rise measured on the two catalysts upon S addition as a function of the corresponding change

in methane conversion with respect to the sulphur-free reaction feed. The data for CPO reaction tests carried out over both catalysts in air follow single straight lines in the whole range explored (0–58 ppm S).

In an adiabatic reactor operation, by assuming a thermal equilibrium between gas and solid (i.e. exit gas temperature is equal to the measured catalyst temperature), a simple heat balance on the gas phase can be written [4]:

$$\Delta H_r^{T_0} = -\frac{W \cdot C_p}{F_{CH_4}} \cdot \left(\frac{\Delta T}{\Delta x_{CH_4}} \right) \quad (3)$$

which relates the variation of temperature ΔT ($^\circ\text{C}$) and methane fractional conversion Δx_{CH_4} to a heat of reaction $\Delta H_r^{T_0}$ (kJ/mol) at the initial temperature T_0 (760°C , for CPO in air over Rh–Pt) through the specific heat of the gas mixture C_p ($0.035 \text{ kJ}/(\text{mol } ^\circ\text{C})$), its total flow rate W (7.22 mol/h) and methane feed flow rate F_{CH_4} (1.64 mol/h). By substituting the value of $\Delta T/\Delta x_{CH_4}$ obtained from the slope of the line in Fig. 10 (-1330°C , over Rh–Pt) into Eq. (3), it results that $\Delta H_r^{760^\circ\text{C}} = +205 \text{ kJ/mol}$, which corresponds reasonably well to the heat of reaction of methane steam reforming at the temperature of 760°C . This value however, is slightly less than that calculated for Rh only sample ($\Delta H_r^{700^\circ\text{C}} = +225 \text{ kJ/mol}$, from CPO data in air [4]) which corresponds perfectly to the heat of reaction of methane steam reforming at 700°C .

These findings confirm that the presence of sulphur in the feed mainly inhibits the steam reforming reaction, which proceeds under kinetic controlled regime in both catalysts [25,26], by selectively poisoning the isolated Rh sites. The small differences in the values of $\Delta H_r^{T_0}$ obtained are in agreement with the larger increase in H_2O production (i.e. lower H_2 selectivity) observed over bimetallic Rh–Pt catalyst.

Under S-free feed Rh is more active than Pt in activating CH_4 molecules [25]; thus the final product distribution is largely affected by the intrinsic high and unmatched selectivity of Rh to H_2 rather than that of Pt. However the selective S adsorption on well-dispersed Rh sites, which has been demonstrated to strongly inhibit the steam reforming reaction, is also likely to slow down the oxidation reactions occurring in the first part of the reactor on those Rh sites. In the monometallic Rh catalyst this is hardly detected from final product of CPO because oxidation reactions are still so fast that their overall rate is controlled by external mass transfer [3,25,26]. On the other hand the activity of Pt sites is almost unaffected by S [3], therefore in the presence of sulphur they can contribute to a larger extent to methane conversion with the consequence of higher selectivity to H_2O (and CO).

4. Conclusions

Catalytic partial oxidation of methane to syngas was investigated over monometallic 1 wt.% Rh and bimetallic Rh–Pt and Rh–Pd catalysts (0.5–0.5 wt.%) prepared by sequential impregnations on commercial $La-\gamma-Al_2O_3$ with the aim of improving the sulphur tolerance of the catalyst while reducing its cost by decreasing the Rh content. Results of CPO light-off, steady state and transient operation under self-sustained, pseudo-adiabatic conditions at short contact time demonstrated that Rh is always the most active and selective element for syngas production from methane in sulphur-free conditions, due to its unique ability to catalyze the steam reforming reaction. However it was shown by DRIFT spectra of adsorbed CO before and after sulphur poisoning that sulphur acts as a selective poison by preferentially adsorbing on smaller well-dispersed Rh crystallites (Rh^+) characterized by $Rh-(CO)_2$ bands while the metallic Rh sites (Rh^0 in larger aggregates) are mostly unaffected. Experiments on Rh catalysts supported on γ - or α -alumina with a large difference in metal dispersion confirmed

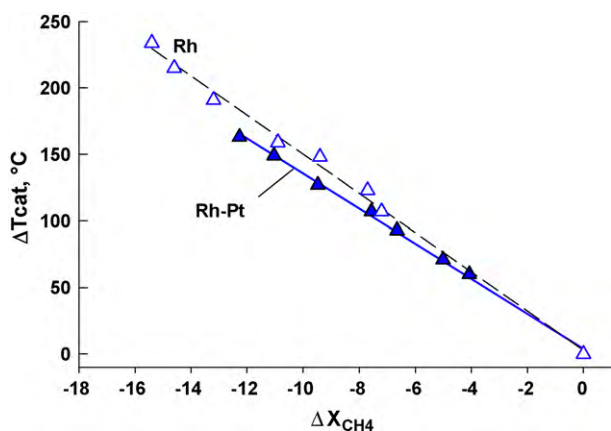


Fig. 10. Increase in catalyst temperature as a function of the variation of methane conversion measured upon the addition of increasing levels of H_2S over Rh–LA and Rh–Pt/LA monolith. $CH_4/O_2 = 2$, air as oxidant, GHSV = $8.1 \times 10^4 \text{ h}^{-1}$.

that S-poisoning of Rh sites is structure-sensitive and is completely reversible under high-temperature reductive conditions. DRIFT experiments indicated the presence of Pt or Pd does not modify the way S interacts and adsorbs on well-dispersed Rh sites. This agrees well with CPO activity data on monometallic Rh catalyst, which showed a rapid and reversible inhibition of the methane steam reforming reaction and a consequent increase in the operating temperature of the system. The impact of S inhibition on Rh was larger at lower temperatures (i.e. higher dilution).

Regarding bimetallic catalyst formulations, Pd was found to have a detrimental effect on the overall catalytic activity and to be ineffective in improving the S-tolerance probably due to its higher sensitivity to S-poisoning than Rh. On the other hand, the partial substitution of Rh with Pt was shown to be effective at reducing and limiting the detrimental impact of S on monometallic Rh catalyst. In the presence of sulphur, the methane conversion is equal or higher on Rh–Pt, the benefit in terms of yields to H₂ and CO being more significant when operating in air, i.e. at higher dilution. The improved performance of the bimetallic Rh–Pt catalyst is due to its higher operating temperature which facilitates sulphur desorption from the catalyst and reduces its accumulation thus resulting in higher catalytic activity and better tolerance against sulphur. The correlation between the loss in the CPO activity in the presence of sulphur and the identification of metal sites most affected by sulphur gives a new insight for designing more efficient and resistant catalysts for the CPO of methane.

References

- [1] M. Lyubovsky, S. Roychoudhury, R. LaPierre, *Catal. Lett.* 99 (2005) 113.
- [2] S. Cimino, G. Landi, L. Lisi, G. Russo, *Catal. Today* 117 (2006) 454.
- [3] A. Bitsch-Larsen, N.J. Degenstein, L.D. Schmidt, *Appl. Catal. B: Environ.* 78 (2008) 364.
- [4] S. Cimino, R. Torbati, L. Lisi, G. Russo, *Appl. Catal. A: Gen.* 360 (2009) 43.
- [5] R. Torbati, S. Cimino, L. Lisi, G. Russo, *Catal. Lett.* 127 (2009) 260.
- [6] A. Shamsi, *Catal. Today* 139 (2009) 268.
- [7] R.K. Kaila, A. Gutiérrez, A.I. Krause, *Appl. Catal. B: Environ.* 84 (2008) 324.
- [8] A.C. McCoy, M.J. Duran, A.M. Azad, S. Chattopadhyay, M.A. Abraham, *Energy Fuels* 21 (2007) 3513.
- [9] J.J. Benitez, I. Carrizosa, J.A. Odrizola, *Appl. Surf. Sci.* 84 (1995) 391.
- [10] E. Finocchio, G. Busca, P. Forzatti, G. Groppi, A. Beretta, *Langmuir* 23 (2007) 10419.
- [11] R. Maurel, G. Leclercq, J. Barbier, *J. Catal.* 37 (1975) 324.
- [12] A. Donazzi, A. Beretta, G. Groppi, P. Forzatti, V. Dal santo, L. Sordelli, V. De grandis, *Proc. 6WCOC, Lille, France, July 5–10, 2009*.
- [13] C. Cao, A. Bourane, J.R. Schlup, K.L. Hohn, *Appl. Catal. A: Gen.* 344 (2008) 78.
- [14] J. Anderson, C. Rochester, Z. Wang, *J. Mol. Catal. A* 139 (1999) 285.
- [15] J.B. Peri, *J. Catal.* 52 (1978) 144.
- [16] J. Anderson, C. Rochester, *J. Chem. Soc., Faraday Trans.* 87 (9) (1991) 1479.
- [17] C.R. Apesteguia, C.E. Brema, T.F. Garetto, A. Borgna, J.M. Parera, *J. Catal.* 89 (1984) 52.
- [18] J.R. Chang, S.L. Chang, *J. Catal.* 176 (1998) 42.
- [19] L.J. Hoyos, M. Primet, H. Praliaud, *J. Chem. Soc., Faraday Trans.* 88 (1992) 3367.
- [20] O. Dulaurent, K. Chandes, C. Bouly, D. Bianchi, *J. Catal.* 188 (1999) 237.
- [21] T. Mailet, J. Barbier, P. Gelin, H. Praliaud, D. Duprez, *J. Catal.* 202 (2001) 367.
- [22] M. Chen, L.D. Schmidt, *J. Catal.* 56 (1979) 198.
- [23] B.M. Joshi, H.S. Gandhi, M. Shelef, *Surf. Coat. Technol.* 29 (1986) 131.
- [24] T.J. Truex, *SAE Paper No. 01-1543* (1999).
- [25] R. Horn, K.A. Williams, N.J. Degenstein, A. Bitsch-Larsen, D. Dalle Nogare, S.A. Tupy, L.D. Schmidt, *J. Catal.* 249 (2007) 380.
- [26] A. Beretta, G. Groppi, M. Lualdi, I. Tavazzi, P. Forzatti, *Ind. Eng. Chem. Res.* 48 (2009) 3825.
- [27] M. Ferrandon, J. Mawdsley, T. Krause, *Appl. Catal. A: Gen.* 342 (2008) 69.
- [28] R.K. Kaila, A. Gutierrez, S.T. Korhonen, A.O. Krause, *Catal. Lett.* 115 (2007) 70.